Temperature-controlled changeable oxygenation selectivity by singlet oxygen with a polymeric photosensitizer†

Hisao Koizumi, Yumi Kimata, Yasuhiro Shiraishi* and Takayuki Hirai

Received (in Cambridge, UK) 5th December 2006, Accepted 22nd January 2007
First published as an Advance Article on the web 12th February 2007
DOI: 10.1039/b617718b

A polymeric photosensitizer, poly(NIPAM-*co*-RB), consisting of *N*-isopropylacrylamide and rose bengal units, demonstrates a temperature-controlled changeable oxygenation selectivity by singlet oxygen in water.

Development of photoreaction systems promoting selective oxidation of molecules with molecular oxygen (O_2) is one of the most important subjects in photochemistry.[1] Substrate- and product-selective oxygenations have been achieved using several organized and constrained media (zeolites, polymers, vesicles, and microemulsions) as "microreactors".[2] These host systems provide cavities and/or surfaces to alter the photochemical behavior of the molecules leading to selective oxygenation. Most of these systems, however, have *unique* selectivity; in other words, the selectivity is basically not changeable. Some systems can change the selectivity by an addition of a third component;[3] however, this results in an *irreversible* change. A photoreaction system, capable of changing the oxygenation selectivity *reversibly* by simple external stimuli without contaminating the system, had not been proposed.

Our photoreaction system presented here promotes a substrate-selective oxygenation in water, whose selectivity is reversibly controlled by *temperature* as the external stimulus. We use a polymeric photosensitizer, poly(NIPAM-*co*-RB), consisting of *N*-isopropylacrylamide (NIPAM)[4] and rose bengal (RB)[5] units as the thermosensitive and photosensitizing parts (Fig. 1A). In that, the photoexcited RB produces a singlet oxygen ($^1O_2$),[6] an oxygenation agent, *via* an energy transfer to O_2 (Fig. 1B). To the best of our knowledge, this is the first reaction system capable of changing the oxygenation selectivity by temperature. It is well-known that polyNIPAM in water shows a reversible *coil*-to-*globule* phase transition, associated with hydration/dehydration of the polymer chain by temperature.[4] Here we describe that this changeable $^1O_2$ oxygenation selectivity is driven by a hydrophobic microenvironment formed inside the polymer behaving as an intelligent microreactor, which promotes a temperature-controlled selective encapsulation/elimination of substrates.

Poly(NIPAM$_x$-*co*-RB$_y$) (x/y = 501/1) was easily synthesized by copolymerization of NIPAM and vinylbenzyl chloride followed by reaction with RB.†‡ Oxygenation selectivity was estimated with a competitive transformation of phenol (**1a**) and 1-naphthol (**2a**) to the corresponding quinones (**1b** and **2b**; Fig. 1B), a typical $^1O_2$ oxygenation reaction.[6] The reaction was carried out by photoirradiation ($\lambda > 530$ nm) to an O_2-saturated aqueous solution (pH 7) containing **1a** and **2a** (each 10 μmol) with poly(NIPAM-*co*-RB) (0.58 mg containing 0.01 μmol RB and 5.01 μmol NIPAM units).†

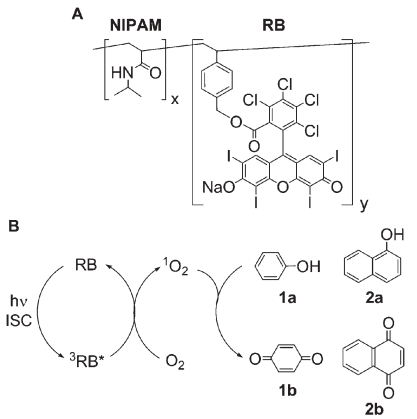

Fig. 1 (A) Structure of poly(NIPAM-*co*-RB), where each unit is randomly arranged along the chain. (B) Sensitized $^1O_2$ oxygenation.

Fig. 2A shows temperature-dependent change in the quinone yields obtained by photoirradiation of **1a** and **2a** together. With RB§ (0.01 μmol) as the sensitizer (white symbols), both **1b** and **2b** yields increase slightly with a rise in temperature, as is usually observed for $^1O_2$ oxygenation.[7] This is because the temperature increase accelerates the diffusion of RB, O_2, and substrates in solution, resulting in an enhancement of $^1O_2$ formation and substrate oxygenation. As summarized in Fig. 2B (white bar), **2b** selectivity [=[**2b**]/([**1b**] + [**2b**]) × 100 (%)] obtained with RB is

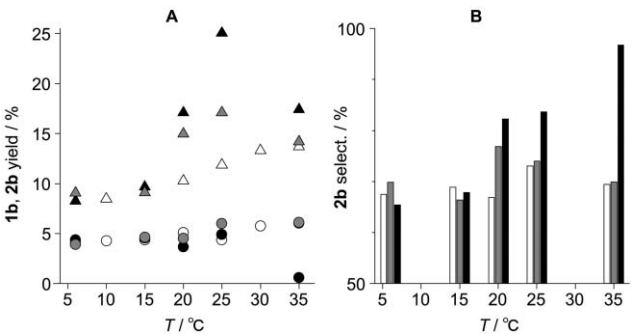

Fig. 2 Temperature-dependent changes in (A) the yields of (circle) **1b** and (triangle) **2b** and (B) the **2b** selectivity [=[**2b**]/([**1b**] + [**2b**]) × 100 (%)], obtained by photoirradiation (0.5 h) of **1a** and **2a** together (each 10 μmol) in O_2-saturated aqueous solution (pH 7). The systems are: (white) with 0.01 μmol RB, (black) with 0.58 mg poly(NIPAM-*co*-RB), and (grey) with 0.01 μmol RB and 0.58 mg polyNIPAM (RB-free).

Research Center for Solar Energy Chemistry, and Division of Chemical Engineering, Graduate School of Engineering Science, Osaka University, Toyonaka, 560-8531, Japan. E-mail: shiraish@cheng.es.osaka-u.ac.jp; Fax: +81-6-6850-6273; Tel: +81-6-6850-6271

† Electronic supplementary information (ESI) available: Materials, methods and figures S1–S7. See DOI: 10.1039/b617718b

almost constant (*ca.* 70%) at the entire temperature range, indicating that the substrate selectivity is not changeable.

As shown in Fig. 2A (black triangle), with poly(NIPAM-*co*-RB), **2b** yield at 5–15 °C is similar to that obtained with RB (white triangle). The **2b** yield, however, increases drastically at 15–25 °C and decreases at >25 °C. In contrast, **1b** yield (black circle) at 5–25 °C is similar to that obtained with RB (white circle), but decreases at >25 °C, resulting in zero yield at 35 °C.[8] As shown in Fig. 2B (black bar), **2b** selectivity at 5–15 °C (*ca.* 70%) is similar to that obtained with RB (white bar), but increases gradually at >15 °C: the value reaches 97% at 35 °C. These indicate that the polymer changes the $^1O_2$ oxygenation selectivity by temperature and oxidizes **2a** very selectively at higher temperature.

This changeable $^1O_2$ oxygenation selectivity of poly(NIPAM-*co*-RB) is driven by a heat-induced phase transition of the polymer from *coil* to *micelle*, and then to *globule* state (Fig. 3). The micelle contains a loosely-aggregated *hydrophobic domain*, while the globule contains a strongly-aggregated *hydrophobic core*. Fig. 4 (white symbol) shows temperature-dependent change in turbidity (A_{650}) of aqueous solution containing poly(NIPAM-*co*-RB); an obvious turbidity increase at >30 °C implies that almost all of the polymer aggregates strongly at >30 °C (globule formation).[9] As shown in Fig. 4 (black symbol), dynamic light scattering (DLS) analysis of the polymer solution detects a scattered light at >25 °C (detection limit, 3 nm), indicating a formation of the hydrophobic core.[10] This implies that strong polymer aggregation occurs partially at >25 °C (Fig. 3). ^{1}H NMR analysis of the polymer dissolved in D_2O (Fig. S2†) shows a gradual decrease in the integrated intensity of C*H* resonance for the polymer chain and the NIPAM unit at 5–25 °C. This indicates that, as described,[11] the hydrophobic domain forms within the polymer at 5–25 °C (micelle formation) and the domain becomes more hydrophobic with a rise in temperature. In contrast, at >25 °C, the signal intensity decreases drastically (Fig. S2†). This is due to a removal of D_2O associated with the strong polymer aggregation (core formation).[10] The temperature-dependent change in the structure of the polymer can therefore be summarized in Fig. 3.

The **2b** yield increase at 15–25 °C (Fig. 2A, black triangle) is driven by the heat-induced growth of the hydrophobic domain, which enhances the **2a** uptake into the polymer. This is confirmed by ^{1}H NMR analysis of **1a** or **2a** in the presence of poly(NIPAM-*co*-RB). Fig. 5A shows change in the spectra of **2a** measured with the polymer for instance. Fig. 5B summarizes change in the

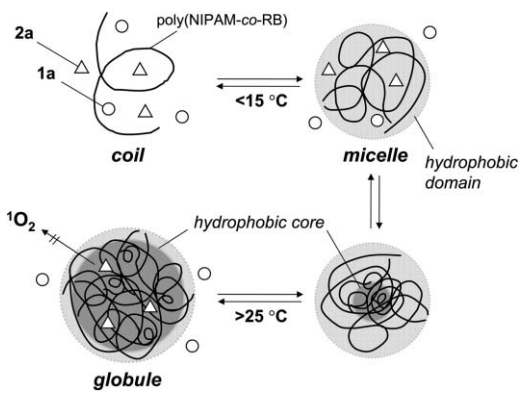

Fig. 3 Schematic representation of temperature-dependent changes in structure of poly(NIPAM-*co*-RB) and in behavior of substrates.

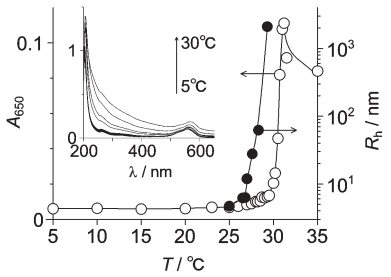

Fig. 4 Change in turbidity (A_{650}) and hydrodynamic radius (R_h) of aqueous solution (pH 7) containing poly(NIPAM-*co*-RB) with temperature. (Inset) Change in absorption spectra of the polymer solution. For detailed R_h data see Fig. S3.†

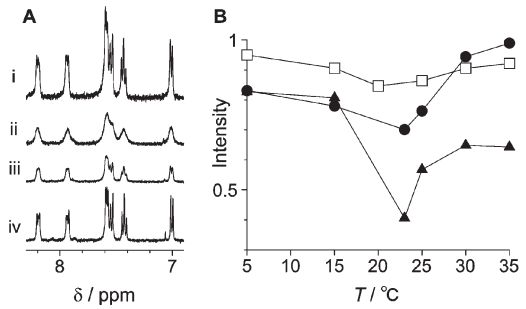

Fig. 5 (A) ^{1}H NMR spectra of **2a** in D_2O measured at (i) 35 °C without polymer and measured at (ii) 35, (iii) 23, and (iv) 5 °C with poly(NIPAM-*co*-RB). (B) Temperature-dependent change in integrated intensity of aromatic C*H* resonance of (black circle) **1a** measured with poly(NIPAM-*co*-RB), (black triangle) **2a** measured with poly(NIPAM-*co*-RB), and (open square) RB measured with RB-free polyNIPAM. The intensities of **1a**, **2a**, and RB measured at 35 °C without polymer are set as 1. The respective ^{1}H NMR spectra for **1a** and RB are shown in Fig. S4.†

integrated intensity of the aromatic C*H* resonance for **1a** or **2a**, where the intensity of **1a** or **2a** measured at 35 °C without the polymer is set as 1. The intensities of both **1a** and **2a** are <1 at 5–15 °C, meaning that a part of **1a** and **2a** exists within the hydrophobic domain of the polymer. At 15–23 °C, decrease in the **2a** intensity is much larger than that of the **1a** intensity, implying that **2a** is encapsulated more within the domain. This is because of higher hydrophobicity of **2a** due to its condensed aromatic rings.[12] The selective accumulation of **2a** within the domain accelerates oxygenation by $^1O_2$ formed within the domain, thus resulting in the **2b** yield increase at 15–25 °C (Fig. 2A, black triangle).

At >25 °C (Fig. 2A, black symbols), both **1b** and **2b** yields obtained with poly(NIPAM-*co*-RB) decrease as the temperature rises. At 35 °C, the **1b** yield is almost zero, although **2b** yield is still higher than that obtained with RB. The **2b** selectivity at 35 °C is 97%, indicating that **2a** oxygenation proceeds very selectively. This high selectivity is explained by the heat-induced phase transition of the polymer from micelle to globule containing a hydrophobic core. As shown in Fig. 5B, the integrated aromatic proton intensity of **1a** and **2a** measured with poly(NIPAM-*co*-RB) increases at >25 °C, which is in accordance with the formation of the hydrophobic core (Fig. 4). This intensity increase is because the strong polymer aggregation (core formation) expels **1a** and **2a** from the polymer. The intensity of **1a** at 35 °C becomes 1, indicating that almost all of **1a** exists in bulk water. At this temperature, **1a** oxygenation by $^1O_2$ must occur in bulk water. Within the

strongly-aggregated core, O_2 can diffuse and form $^1O_2$.[13] However, diffusion of $^1O_2$ to bulk water is strictly limited by the rigid core.[14] As shown in Fig. 4, the size of the core increases exponentially as the temperature rises, indicating that $^1O_2$ diffusion to bulk water is restricted more. These suggest that **1b** yield decreases at >25 °C (Fig. 2A, black circle) because **1a** is expelled from the polymer and the diffusion of $^1O_2$ to bulk water is limited.

In contrast, as shown in Fig. 2A (black triangle), the **2b** yield decreases at >25 °C, but the yield at 35 °C is still higher than that obtained with RB. As shown in Fig. 5B, the integrated proton intensity of **2a** obtained with the polymer increases at >25 °C, as is also the case for **1a**, but is saturated at around 0.65. This means that **2a** still exists within the core even at 35 °C, although **1a** is expelled completely from the core. This is due to the higher hydrophobicity of **2a**.[12] The selective **2a** encapsulation to the core therefore promotes selective oxygenation of **2a** at 35 °C (Fig. 2B, black bar). These indicate that the hydrophobic microenvironment formed within the polymer determine the hydrophobicity difference between **1a** and **2a**, thus triggering the temperature-controlled changeable oxygenation selectivity.

It is notable that the copolymerization of the RB units with NIPAM units is necessary for onset of the changeable oxygenation selectivity. Fig. 2A (gray symbols) shows **1b** and **2b** yields obtained by photoirradiation of **1a**, **2a**, and RB, together with RB-free polyNIPAM.¶ The **2b** yield (gray triangle) increases at 15–25 °C, as is also the case with poly(NIPAM-*co*-RB) (black triangle), but the rate of increase is much smaller. As shown in Fig. 5B (white square), integrated proton intensity of RB measured with polyNIPAM decreases only slightly at 15–25 °C. This means that RB is scarcely encapsulated within the hydrophobic domain of polyNIPAM. The absence of RB within the domain cancels the **2a** accumulation, resulting in smaller **2b** yield increase at 15–25 °C. As shown in Fig. 2A (gray circle), **1b** yield is similar to that obtained with RB (white circle) at the entire temperature range. The **1a** oxygenation still occurs at 35 °C, although poly(NIPAM-*co*-RB) suppresses completely (black circle). As shown in Fig. 5B, at 35 °C, almost all of RB exists in bulk solution as well as **1a**, thus allowing the **1a** oxygenation by $^1O_2$ in bulk water. As a result of this, RB with polyNIPAM system does not show temperature-controlled changeable selectivity (Fig. 2B, gray bar).

Fig. 6 shows time-course variation in the **1b** and **2b** yields and the **2b** selectivity obtained with poly(NIPAM-*co*-RB), where the reaction temperature is changed after each 10 min (5 → 35 → 5 °C). The data (white symbols and bars) clearly show that the polymer can control the selectivity *reversibly* by temperature. Another notable feature of the polymer is the high reusability with a simple recovery process: heating the reaction mixture to 40 °C followed by centrifugation (5 min, 2×10^4 rpm) affords >98% polymer recovery, and the recovered polymer (black symbols and bars) shows the same activity as does the virgin polymer.

In summary, we found that a polymeric sensitizer, poly(NIPAM-*co*-RB), reversibly controls the $^1O_2$ oxygenation selectivity by temperature. This unprecedented photosensitizing activity is driven by a heat-induced self-assembly of the polymer, which promotes selective encapsulation/elimination of substrates. The results presented here may contribute to the development of selective photooxygenation processes and to the design of more efficient photosensitizing materials.

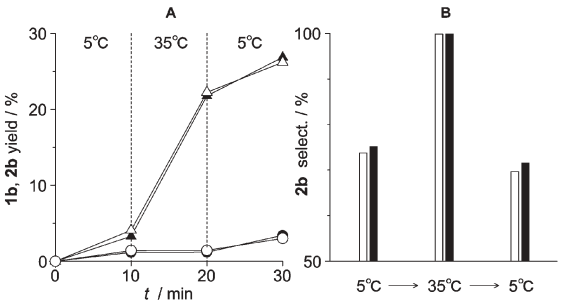

Fig. 6 Changes (A) in the yields of (circle) **1b** and (triangle) **2b** and (B) **2b** selectivity with time in poly(NIPAM-*co*-RB) system, where the reaction temperature is changed after each 10 min (5 → 35 → 5 °C). The data shown by white symbols and bars (run (a)) were obtained using the virgin polymer. The data shown by black symbols and bars were obtained using the polymer recovered after run (a). The recovery process is: heat the sample to 40 °C, followed by centrifugation (5 min, 2×10^4 rpm).

This work was supported by the Grant-in-Aid for Scientific Research (No. 15360430) and that on Priority Area (417; No. 17029037) from the Ministry of Education, Culture, Sports, Science and Technology, Japan (MEXT).

Notes and references

‡ Poly(NIPAM-*co*-RB): M_n = 55000; M_w/M_n = 2.6; E_S (E_T) = 211 (170) kJ mol^{-1}; Φ_{fl} (298 K) = 0.063; Φ_{phos} (77 K) = 0.0017; T_{LCST} = 30 °C.
§ RB: E_S (E_T) = 211 (170) kJ mol^{-1}; Φ_{fl} (298 K) = 0.042; Φ_{phos} (77 K) = 0.0007.
¶ RB-free polyNIPAM: M_n = 35000; T_{LCST} = 31 °C (Fig. S5 and S6†).

1 A. Maldotti, A. Molinari and R. Amadelli, *Chem. Rev.*, 2002, **102**, 3811.
2 (*a*) C.-H. Tung, L.-Z. Wu, L.-P. Zhang and B. Chen, *Acc. Chem. Res.*, 2003, **36**, 39; (*b*) V. Ramamurthy, J. Shailaja, L. S. Kaanumalle, R. B. Sunoj and J. Chandrasekhar, *Chem. Commun.*, 2003, 1987; (*c*) A. Corma and H. Garcia, *Chem. Commun.*, 2004, 1443; (*d*) R. S. H. Liu and G. S. Hammond, *Acc. Chem. Res.*, 2005, **38**, 396.
3 (*a*) K. Wada, H. Yamada, Y. Watanabe and T. Mitsudo, *J. Chem. Soc., Faraday Trans.*, 1998, **94**, 1771; (*b*) P. Boarini, V. Carassiti, A. Maldotti and R. Amadelli, *Langmuir*, 1998, **14**, 2080; (*c*) C. B. Almquist and P. Biswas, *Appl. Catal. A*, 2001, **214**, 259.
4 (*a*) X. Ma, J. Xi, X. Huang, X. Zhao and X. Tang, *Mater. Lett.*, 2004, **58**, 3400; (*b*) J. X. Zhang, L. Y. Qiu, Y. Jin and K. J. Zhu, *Colloids Surf. B*, 2005, **43**, 123; (*c*) R. Motokawa, K. Morishita, S. Koizumi, T. Nakahira and M. Annaka, *Macromolecules*, 2005, **38**, 5748.
5 (*a*) E. C. Blossey, D. C. Neckers, A. L. Thayer and A. P. Schaap, *J. Am. Chem. Soc.*, 1973, **95**, 5820; (*b*) D. C. Neckers, E. C. Blossey and A. P. Schaap, *US. Pat.*, 4 315 998, 1982.
6 (*a*) R. Gerdes, D. Wöhrle, W. Spiller, G. Schneider, G. Schnurpfeil and G. Schulz-Ekloff, *J. Photochem. Photobiol. A: Chem.*, 1997, **111**, 65; (*b*) D. Madhavan and K. Pitchumani, *J. Photochem. Photobiol. A: Chem.*, 2002, **153**, 205.
7 R. Alcántara, L. Canoira, P. G. Joao, J. G. Rodriguez and I. Vázquez, *J. Photochem. Photobiol. A: Chem.*, 2000, **133**, 27.
8 Similar behaviors are observed when **1a** and **2a** are photoirradiated separately (Fig. S1†).
9 C. Wu and X. Wang, *Phys. Rev. Lett.*, 1998, **80**, 4092.
10 Z. Cao, W. Liu, P. Gao, K. Yao, H. Li and G. Wang, *Polymer*, 2005, **46**, 5268.
11 H. G. Schild and D. A. Tirrell, *Langmuir*, 1991, **7**, 1319.
12 The log *P* values for **1a** and **2a**, calculated by ChemDraw Ultra 7.0 software, are 1.64 and 2.64, respectively.
13 H. Ito, T. Ikeda and K. Ichimura, *Macromolecules*, 1993, **26**, 4533.
14 J. W. Snyder, I. Zebger, Z. Gao, L. Poulsen, P. K. Frederiksen, E. Skovsen, S. P. Mcilroy, M. Klinger, L. K. Andersen and P. R. Ogilby, *Acc. Chem. Res.*, 2004, **37**, 894.

